ACS Sustainable Chemistry & Engineering

Research Article

pubs.acs.org/journal/ascecg

Improved Methane Hydrate Formation and Dissociation with Nanosphere-Based Fixed Surfactants As Promoters

Fei Wang,[†,‡] Guo-Qiang Liu,[§] Han-Lin Meng,[∥] Gang Guo,[†] Sheng-Jun Luo,*[,†] and Rong-Bo Guo*[,†]

[†]Shandong Industrial Engineering Laboratory of Biogas Production & Utilization, Key Laboratory of Biofuels, Qingdao Institute of Bioenergy and Bioprocess Technology, Chinese Academy of Sciences, Qingdao 266101, Shandong, China

[‡]University of Chinese Academy of Science, Beijing 100049, China

[§]Qingdao University of Science & Technology, Qingdao 266042, China

[∥]Ocean University of China, Qingdao 266110, China

Supporting Information

ABSTRACT: The fixation of surfactants is very important in surfactant-promoted gas hydrate formation. In this work, three surfactants were fixed on the surface of polystyrene nanospheres through emulsion polymerization (named as Surfactant@PSNS) and then used in methane hydrate formation and dissociation, which were sodium dodecyl sulfate (SDS), cetyltrimethylammonium bromide (CTAB), and dodecyl alcohol ethoxylates (AEO). The fixation of the surfactants could reduce the induction periods and improve the apparent densities and storage capacities of the formed hydrates, especially at low surfactant concentrations. During hydrate dissociation, the fixation of surfactants resulted in the hydrates dissociating more slowly. The methane recoveries were improved from 76.37%, 27.87%, and 32.35% to 87.55%, 43.43%, and 60.20% for the fixation of SDS, CTAB, and AEO, respectively. Moreover, with surfactants fixed, the foam generation during hydrate dissociation was obviously controlled.

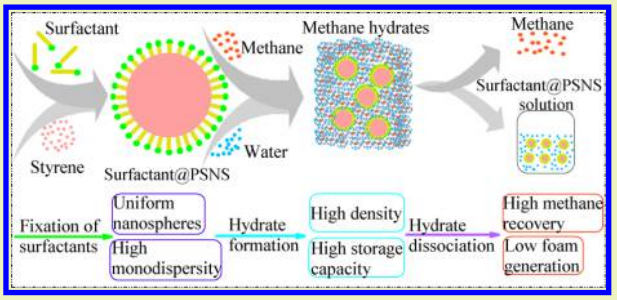

KEYWORDS: *Methane hydrates, Hydrate formation and dissociation, Surfactants, Polystyrene nanospheres, Methane recovery*

INTRODUCTION

Natural gas hydrates are clathrate crystalline compounds formed by water and natural gas molecules under appropriate pressure and temperature.[1] The high storage capacity and good security endow gas hydrates with great potential in natural gas storage and transportation.[2,3] However, several problems have to be solved to utilize the potential of gas hydrates in natural gas storage and transportation, such as the long induction period and low growth rate during hydrate formation.[4,5]

During the past few decades, surfactants have been reported by many researchers as promoters in gas hydrate formation,[6−16] which are of great significance to the industrial application of hydrate-based gas storage and transportation. However, there are also several defects existing in the application of surfactants in gas hydrate formation. On one hand, even though many kinds of surfactants have been used as promoters in gas hydrate formation, only anionic ones, especially sodium dodecyl sulfate (SDS), showed the most efficient promotion, while cationic and anionic surfactants produced obviously less efficient promotion compared with anionic ones.[7,12,13] On the other hand, many surfactants showed very low solubilities under hydrate formation conditions,[8] which might limit the application of surfactants in gas hydrate formation. In addition, the existence of surfactants would lead to a lot of foam generated during the hydrate dissociation, which not only caused the outflow of surfactants but impacted the application of hydrates. Therefore, overcoming the defects and improving the application of surfactants in promoting gas hydrate formation are of great significance in the field of hydrate-based gas storage and transportation.

Recently, many researchers have reported to improve gas hydrate formation by confining the reaction solution in the fixed bed with nano/microporous material, such as active carbon and silica sands.[17−19] With the reaction solution dispersed in the nano/microstructures, gas hydrate formation could be improved efficiently. In addition, the reaction solutions were also used in the form of dry water to enhance gas hydrate formation,[20,21] in which the water existed as micro droplets, as a result, a very rapid hydrate formation and high storage capacity were achieved. However, the hydrate dissociation might result in the aggregation of the dry water powders and therefore led to poor recycling performance of dry water in gas hydrate formation.

In our previous work,[22] we fixed anionic surfactant SDS on the surface of polystyrene nanospheres (name as SDS@PSNS) through emulsion polymerization and then used the fixed SDS

Received: November 23, 2015
Revised: February 17, 2016
Published: March 14, 2016

DOI: 10.1021/acssuschemeng.5b01557
ACS Sustainable Chem. Eng. 2016, 4, 2107−2113

as promoters in methane hydrate formation, as a result, the fixed SDS led to shorter induction periods and higher methane consumption during hydrate formation and less foam generated during hydrate dissociation. However, only SDS was used for the fixation of surfactants and both SDS and SDS@PSNS were used in methane hydrate formation only at low concentrations (0.5−2 mmol/L). In the present work, to further study the application of the fixation of surfactants in hydrate-based gas storage and transportation, different surfactants, anionic SDS, cationic CTAB, and nonionic AEO were fixed on the surface of polystyrene nanospheres and then used as promoters in methane hydrate formation. To evaluate the effects of the fixation of surfactants on methane hydrate formation more comprehensively, both the surfactants and the Surfactant@PSNSs were used at a wider concentration range (1−8 mmol/L). Moreover, the hydrate dissociation was also studied.

EXPERIMENTAL SECTION

Materials. Sodium dodecyl sulfate (SDS, A.R.) was provided by Sinopharm Chemical Reagent Co., Ltd. (Shanghai, China). Cetyltrimethylammonium bromide (CTAB, A.R.) was purchased from Shanghai Aibi Chemistry Co., Ltd. (Shanghai, China). Dodecyl alcohol ethoxylates (AEO, purity >99%) were provided by Qingdao Changxing Chemical Co., Ltd. (Qingdao, China). Styrene (A.R.) was purchased from Tianjin Guangcheng Chemical Reagent Co., Ltd. (Tianjin, China). Anionic initiator ammonium persulfate (APS, A.R.) was purchased from Hengxing Chemical Reagent Co., Ltd. (Tianjin, China). Cationic initiator 2,2′-azobis(N,N′-dim-ethylenisobuyramidine) dihydrochloride (AIBA, purity >98%) was provided by Qingdao Kexin New Material Co., Ltd. (Qingdao, China). Methane and nitrogen with a purity of 99.99% were provided by Heli Gas Co., Ltd. (Qingdao, China). Pyrene (purity ≥99%) was purchased from Sigma. The molecular structures of the surfactants used in this work were shown in Figure S1 (SI).

CMCs and Solubilities of the Surfactants. CMCs (critical micelle concentration) of SDS and CTAB at room temperature (298.15 K) and hydrate formation temperature (275.15 K) were measured via conductometry.[23,24]

CMCs of AEO at 298.15 and 275.15 K were measured through steady-state pyrene fluorescence spectra.[25]

Photos of the surfactant solutions at different concentrations were taken under 298.15 and 273.15 K, which were used together with the conductivity for solubility measurement.

Preparation of Surfactant@PSNS. Surfactant@PSNS was prepared through nitrogen-protected emulsion polymerization with styrene as a monomer and different surfactants as emulsifiers. For anionic emulsion polymerization, APS was used as an initiator, while in cationic and nonionic emulsion polymerization AIBA was used as an initiator. The recipes and conditions for the emulsion polymerization are shown in Table S1 (SI), and the details of the emulsion polymerization are according to Wang and Fang.[26]

Characterization of Surfactant@PSNS. The morphology of Surfactant@PSNS was determined through JEM-1200EX Transmission Electron Microscopy (TEM, Japan Electronics Co., Ltd.).

The average particle size and particle size distribution index (PDI) of Surfactant@PSNS were measured by a Malvern Nano-s90 Laser Particle Size Analyzer (Malvern, UK).

Methane Hydrate Formation. The schematic diagram of the methane hydrate formation apparatus is shown in Figure S2 (SI). The main part of the apparatus consisted of a 350 mL stainless steel reactor equipped with magnetic coupling stirrer (0−1000 rpm) and a wall jacket connected to the cool bath (253.15−373.15 K). Both the reactor and stirrer were made of 316L stainless steel, and the roughness was less than 0.2 μm. The reactor was initially washed with deionized water three times and then purged with methane three times. Afterward, 50 mL of reaction solution was added, and cooling was started. After the reaction temperature (275.15 K) was reached, the reactor was pressurized with methane to the reaction pressure (6 MPa, gauge pressure), and the stirring rate was 200 rpm. All the hydrate formation processes were carried out for 1200 min, and the temperature and pressure of the reaction system were recorded on the computer.

In hydrate-based gas storage and transportation, the gas hydrates are usually separated from the unreacted solution and then compacted for storage and transportation. Therefore, the gas storage capacity of the formed gas hydrates is an important parameter in the application of gas hydrates. In this work, the unreacted solution was discharged through the outlet at the bottom of the reactor after the completion of hydrate formation, and then the volume of the unreacted solution was measured for the calculation of the gas storage capacity of the formed gas hydrates.

The methane consumption at time t is defined as n_t and calculated by eqs 1 and 2, which were derived in our previous study:[22]

$$n_t = \frac{\frac{P_0V_0}{z_0RT_0} - \frac{P_tV_0}{z_tRT_t}}{1 - \frac{P_t\Delta Vm}{z_tRT_t}} \tag{1}$$

$$z_t = 1 + \left[0.083 - 0.422 \times \left(\frac{T_c}{T_t}\right)^{1.6}\right]\frac{P_tT_c}{P_cT_t} + \omega\left[0.139 - 0.172 \times \left(\frac{T_c}{T_t}\right)^{4.2}\right]\frac{P_tT_c}{P_cT_t} \tag{2}$$

where P_0 and P_t are the pressure at time 0 and t; V_0 and V_t are the volume of the gas phase at time 0 and t; T_0 and T_t are the temperature at time 0 and t; R is the universal gas constant; m is the hydration number;[27] ΔV is the molar volume difference between methane hydrates and water, which has been reported as 4.6 cm^3 per mole of water;[28] z_0 and z_t are the compressibility factor at time 0 and t; and for methane, T_c, P_c, and ω are 190.6 K, 4.599 MPa, and 0.012, respectively.[29]

Then the storage capacity (c_s) of formed methane hydrates at time t can be calculated as follows:

$$c_s = \frac{n_t \times V_{mg} \times V_{mw}}{(V_i - V_u) \times (V_{mw} + \Delta V)} = \frac{\frac{P_0V_0}{z_0RT_0} - \frac{P_tV_0}{z_tRT_t}}{1 - \frac{P_t\Delta Vm}{z_tRT_t}} \times \frac{V_{mg} \times V_{mw}}{(V_i - V_u) \times (V_{mw} + \Delta V)} \tag{3}$$

where V_{mg} and V_{mw} are the molar volumes of gas and water respectively; V_i and V_u are the volumes of the initial reaction solution and the unreacted reaction solution, respectively.

Methane Hydrate Dissociation. As mentioned above, the formed hydrates are usually separated from the unreacted water and then compacted for storage and transportation. However, the gas leaks easily from the hydrates during the depressurization, separation, and compaction process, resulting in low gas recoveries of the formed hydrates. In this work, the effects of the fixation of surfactants on the methane recovery were studied, which was defined as the molar ratio of the gas recovered from the obtained hydrates and the methane finally consumed in the gas hydrate formation.

After the methane hydrate formation, the stirring was stopped and the reactor was depressurized to atmospheric pressure rapidly. Then the hydrate dissociation was carried out in the reactor at 275.15 K, and the hydrate dissociation rate and methane recovery were determined.

The amount of methane at time t during the dissociation was defined as n_{dt} and calculated by formula 4, the derivation process of which is shown in the Supporting Information (SI):

$$n_{dt} = \frac{P_{dt} \times (V_0 - n_f \times m \times \Delta V)}{z_{dt} \times R \times T_{dt} - m \times \Delta V \times P_{dt}} \tag{4}$$

where P_{dt} is the reactor pressure at time t during hydrate dissociation, T_{dt} is the reactor temperature at time t during hydrate dissociation, n_f is the final methane consumption during methane hydrate formation,

DOI: 10.1021/acssuschemeng.5b01557
ACS Sustainable Chem. Eng. 2016, 4, 2107−2113

V_0 is the volume of gas phase at time 0 during hydrate formation, ΔV is the molar volume difference between methane hydrates and water, m is the hydration number, R is the universal gas constant, and z_{dt} is the compressibility factor at time t during hydrate dissociation, which is calculated according to formula 2.

Then the methane recovery (r) can be calculated by

$$r = \frac{n_{dt}}{n_f} \times 100\% \quad (5)$$

where n_f is the final methane consumption during the methane hydrate formation process.

In addition, to study the effects of the fixation of surfactants on the foam generation during hydrate dissociation, methane hydrates were taken out immediately after hydrate formation and put into the measuring cylinder with 50 mL of deionized water to make the hydrates dissociate rapidly. Photos were taken after the completion of hydrate dissociation.

RESULTS AND DISCUSSION

CMCs and Solubilities of the Surfactants. The CMCs and solubilities of SDS and CTAB were determined according to the conductivity vs concentration curves and the photos of the surfactant solutions shown in Figure S3 (SI). For SDS, as discussed in our previous study,[30] the CMC at 298.15 K (CMC298.15K SDS) and the solubility at 275.15 K (C275.15K SDS) were regarded as 8.2 and 4.4 mmol/L, respectively. For CTAB at 298.15 K, the flex point of the conductivity vs concentration curve appeared at 1.3 mmol/L, and no precipitation was observed. Therefore, CMC298.15K CTAB was determined as 1.3 mmol/L. At 275.15 K, two flex points (1.1 and 3.4 mmol/L) appeared on the conductivity vs concentration curve, and obvious precipitation took place at 4 mmol/L. Therefore, 1.1 and 3.4 mmol/L were considered as the CMC275.15K CTAB and C275.15K CTAB, respectively.

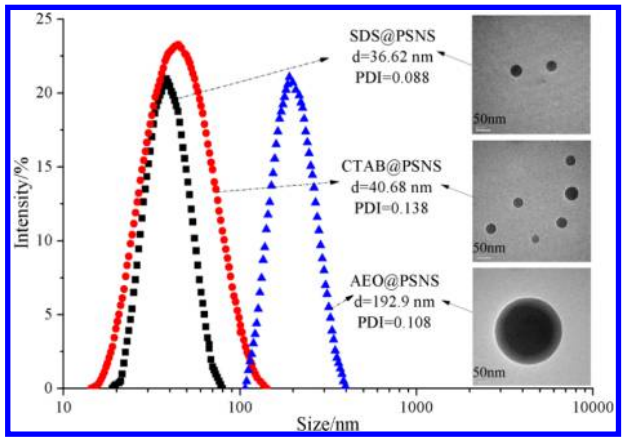

Figure 1. Particle sizes, particle size distribution indexs (PDI), and TEM photos of Surfactant@PSNS.

The CMCs of AEO were measured by pyrene fluorescence spectra shown in Figure S3. The intensity ratio of the first peak (I_1, λ = 374 nm) and the third peak (I_3, λ = 384 nm) of the pyrene fluorescence emission spectra could denote the polarities of the microdomains.[25] According to Aguiar et al.,[31] the midpoint of the decreasing part of I_1/I_3 vs concentration curve could be considered as the CMC. In this work, the midpoints of the linear fits of the decreasing parts of I_1/I_3 vs concentration curves appeared at about 0.45 and 0.95 mmol/L at 298.15 and 275.15 K, respectively. Therefore, the CMC298.15K AEO and CMC275.15K AEO were regarded as 0.45 and 0.95 mmol/L, respectively.

Characterizations of Surfactant@PSNS. Figure 1 shows the TEM photos, particle sizes, and particle size distributions of the Surfactant@PSNS particles, which indicated that the Surfactant@PSNS particles appeared as monodispersed uniform spheres on the nanoscale. In the emulsion polymerization with nonpolymerizable surfactants, such as SDS, CTAB, and AEO, polystyrene nanospheres were achieved through a micelle nucleation mechanism.[26] First, micelles were formed with surfactant molecules in the aqueous phase, and then the monomer molecules could diffuse into the micelles under stirring, resulting in the formation of monomer-swollen micelles. Afterward, free radicals generated from the pyrolysis of initiator molecules could spread into the monomer-swollen micelles and initiated the polymerization, leading to the continuous formation of polystyrene macromolecules in the monomer-swollen micelles. The macromolecules could twine with each other and make the surfactant carbon chains embeded in the macromolecules. Therefore, it could be imagined that the surfactants were fixed uniformly on the

Table 1. Induction Time of Methane Hydrate Formation with Different Reaction Solutions[a]

surfactant	c (mmol/L)	induction time/min			surfactant @PSNS	c^b (mmol/L)	induction time/min		
		1	2	3			1	2	3
DI water		-[c]	-	-					
SDS	1	347	-	485	SDS@PSNS	1	135	132	279
	2	186	561	399		2	82	148	129
	4	76	-	103		4	196	23	17
	8	-	140	-		8	150	12	83
CTAB	1	-	-	-	CTAB@PSNS	1	290	203	248
	2	538	204	254		2	118	213	185
	4	243	-	197		4	160	290	179
	8	309	-	316		8	107	265	128
AEO	1	451	621	675	AEO@PSNS	1	255	341	435
	2	506	575	-		2	300	234	436
	4	-	338	367		4	316	119	132
	8	590	435	916		8	480	177	167

[a]The initial conditions were 6 MPa and 275.15 K. [b]The concentration of Surfactant@PSNS was determined as the overall concentration of surfactants in the Surfactant@PSNS solution. [c]"-" indicates that on obvious hydrate formation was observed within 1200 min.

DOI: 10.1021/acssuschemeng.5b01557
ACS Sustainable Chem. Eng. 2016, 4, 2107−2113

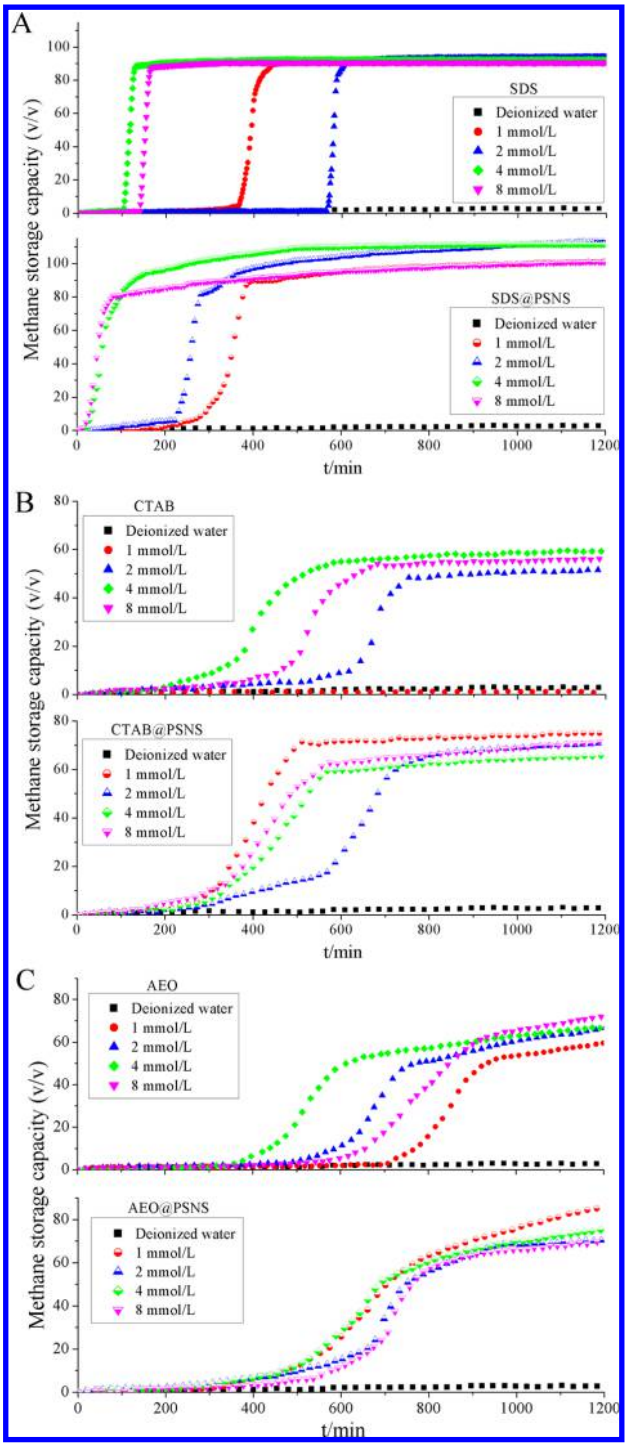

Figure 2. Methane consumptions in hydrate formations with different promoters (the initial conditions were 6 MPa and 275.15 K).

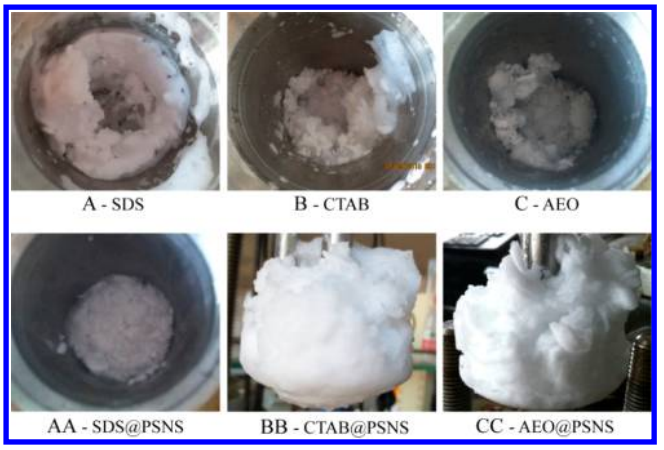

Figure 3. Morphologies of methane hydrates formed with different promoters (all promoters were used at 2 mmol/L; the initial conditions were 6 MPa and 275.15 K).

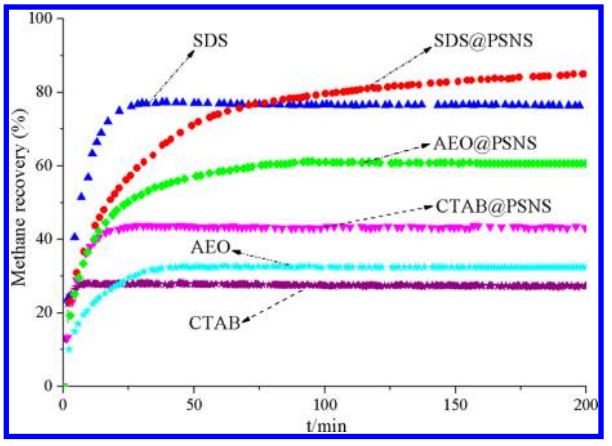

Figure 4. Dissociation rates of the methane hydrates formed with different promoters (all the promoters were used at 2 mmol/L; the hydrate dissociation was carried out at 275.15 K).

Table 2. Methane Consumption and Recovery of Hydrates Formed with Different Promoters[a]

promoters	c (mmol/L)	methane consumed (mol)	methane recovered (mol)	methane recovery (%)
SDS	2	0.237	0.181	76.37
SDS@PSNS	2	0.265	0.232	87.55
CTAB	2	0.122	0.034	27.87
CTAB@PSNS	2	0.175	0.076	43.43
AEO	2	0.136	0.044	32.35
AEO@PSNS	2	0.201	0.121	60.20

[a]Initial pressure of hydrate formation was 6 MPa; both the hydrate formation and dissociation temperature were 275.15 K.

surface of polystyrene nanospheres in the Surfactant@PSNS solutions.

Induction Time. Table 1 shows the induction times of methane hydrate formations with different promoters, which was considered as the time from charging gas into the reactor to the time an obvious temperature spike was observed.[32] Each hydrate formation experiment was carried out three times given the stochasticity of hydrate nucleation. When pure deionized water (DI water) was used, no obvious hydrate formation was observed within 1200 min, while both surfactants and Surfactant@PSNSs produced efficient promotion to methane hydrate formation. Table 1 also shows that Surfactant@PSNSs led to shorter induction periods compared with the corresponding surfactants, especially when taking into account that no hydrate formation was observed within 1200 min for many experiments with surfactants. At low concentrations of surfactant solutions (1−2 mmol/L), as surfactant molecules dispersed in the aqueous phase, the surfactants might be too

DOI: 10.1021/acssuschemeng.5b01557
ACS Sustainable Chem. Eng. 2016, 4, 2107−2113

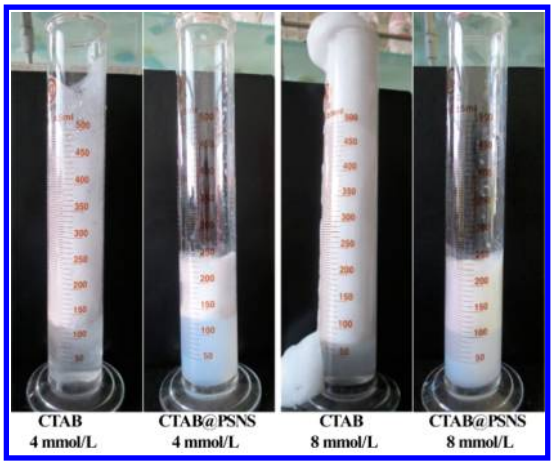

Figure 5. Dissociation morphologies of hydrates formed with different reaction solutions (the dissociation was carried out at room temperature).

dilute to lead to fast hydrate nucleation. While in the Surfactant@PSNS solutions, with the surfactant molecules arranged on the surface of polystyrene nanospheres, much higher microscopic surfactant densities were obtained, which showed better promotion to hydrate nucleation and therefore led to shorter induction periods. At high concentrations of surfactant solutions (4−8 mmol/L), as shown in Figure S3, surfactant molecules precipitated obviously from the solutions. While the Surfactant@PSNS particles still dispersed in the SDS@PSNS solutions stably, the surfactant molecules arranged on the surface of SDS@PSNS particles uniformly with high density. As a result, shorter induction periods with the Surfactant@PSNS solutions were achieved.

Methane Hydrate Formation Rate. Figure 2 shows the methane consumptions in hydrate formations with different promoters. Surfactant@PSNSs produced slight priority over the corresponding surfactants on the methane consumption, which indicated that Surfactant@PSNSs led to the hydrates formed with slightly higher storage capacity. For anionic promoters, when SDS was used, hydrates initially formed on the reactor sidewall and then grew upward on the reactor sidewall.[10] Afterward, the reaction solutions could be sucked to the hydrate surface under capillary effect to keep continuous gas−liquid contact;[9] as a result, hydrate growth was completed rapidly within about 40 min (Figure 2A). However, the formed hydrates accumulated loosely on the reactor sidewall until the upper edge, as shown in Figure 3. When SDS@PSNS was used, hydrates mainly formed in the bulk of the solution with SDS@PSNS particles as media, and the continuous growth and agglomeration of the formed hydrates led to the completion of hydrate formation.[22] Consequently, even with slightly slower hydrate growth, the hydrates formed with SDS@PSNS accumulated compactly in the bottom of the reactor with higher storage capacity (Figures 2 and 3). For cationic and nonionic promoters, as shown in Figure 3, both the surfactants and Surfactant@PSNSs did not lead to upward hydrate growth on the reactor sidewall, which denoted that the hydrates formed in the bottom of the reactor. However, hydrates existed in the reactor loosely when CTAB and AEO were used, while CTAB@PSNS and AEO@PSNS led to the hydrates formed around the stirrer more compactly with higher methane storage capacity (Figures 2 and 3).

Methane Hydrate Dissociation. Figure 4 shows the dissociation rates of the methane hydrates formed with different promoters. Surfactant@PSNSs resulted in a lower hydrate dissociation rate compared with the corresponding surfactants. On one hand, as shown in Figure 2 and Table 2, Surfactant@PSNSs led to more methane consumed during gas hydrate formation, which meant that more hydrates formed with Surfactant@PSNSs. Then during the dissociation period, more hydrates led to more heat absorbed due to the endothermic feature of hydrate dissociation and therefore resulted in low temperature, which in turn caused the lower dissociation rates. On the other hand, as shown in Figure 3, surfactants led to the methane hydrates formed in the reactor loosely, which indicated that the hydrates could dissociate more easily during the dissociation process, leading to the higher dissociation rates of methane hydrates formed with surfactants. However, the loose structures and faster hydrate dissociation of the methane hydrates formed with surfactants might also lead to the gas leaking easily from hydrates during the storage and transportation; therefore, the hydrates formed with Surfactant@PSNSs were more applicable for gas storage and transportation due to the higher density and lower dissociation rates.

Figure 4 also shows that Surfactant@PSNSs led to higher methane recoveries compared with corresponding surfactants. In this work, the reactor was depressurized rapidly until atmospheric pressure after hydrate formation, and then the hydrates were dissociated in the reactor. When surfactants were used, hydrates formed in the reactor loosely; therefore, methane might be easily released from the hydrates during the depressurization process, leading to low methane recoveries. However, when the surfactants were fixed on the surface of polystyrene nanospheres, methane hydrates were formed more compactly, and the gas was not easy to release during the depressurization. As a result, the methane recoveries were improved from 76.37%, 27.87%, and 32.35% to 87.55%, 43.43%, and 60.20% for ionic, cationic, and anionic promoters, respectively, as shown in Table 2.

Figure 5 shows the dissociation morphologies of hydrates formed with CTAB and CTAB@PSNS. When CTAB was used, a lot of foam was generated during the hydrate dissociation, and higher surfactant concentration led to more foam generated. As shown in Figure 5, the foam even spilled from the measuring cylinder during the dissociation of hydrates formed with CTAB of 8 mmol/L, which not only led to the loss of surfactants but also affected the application of the gas hydrates. However, when surfactants were fixed on the surface of polystyrene nanospheres, the foam generation was obviously restrained, as shown in Figure 5. During the dissociation of hydrates formed with surfactants, the hydrates dissociated into water, and the surfactant molecules could dissolve into the water, forming surfactant solutions on the hydrate surface. Then, with the dissociation of hydrates, gas was released continuously, resulting in the generation of lots of foam. When CTAB@PSNS was used, as the surfactants were fixed, no surfactant solutions were formed during the hydrate dissociation. As a result, the generation of foam was obviously controlled, which could not only inhibit the loss of surfactants but also be conducive to the recycling of CTAB@PSNS in methane hydrate formation and dissociation.

CONCLUSIONS

Nanosphere-based fixation of surfactants (SDS, CTAB, and AEO) was applied in methane hydrate formation and

DOI: 10.1021/acssuschemeng.5b01557
ACS Sustainable Chem. Eng. 2016, 4, 2107−2113

dissociation. Compared with the free surfactants, the fixed surfactants (Surfactant@PSNS) resulted in shorter induction periods of hydrate formation and higher storage capacities of the formed hydrates, especially at low surfactant concentrations. In addition, Surfactant@PSNS led to the hydrates formed with higher apparent density. During hydrate dissociation, the fixed surfactants resulted in slower dissociation rates and obviously higher methane recoveries. Moreover, with surfactants fixed, the foam generation was obviously controlled during the hydrate dissociation. Given the high hydrate apparent density during hydrate formation and low foam generation during hydrate dissociation, Surfactant@PSNS was of significant potential in hydrate-based natural gas storage and transportation.

■ ASSOCIATED CONTENT

Supporting Information

The Supporting Information is available free of charge on the ACS Publications website at DOI: 10.1021/acssuschemeng.5b01557.

The molecular structures of the surfactants; the schematic diagram of the methane hydrate formation apparatus; the conductivity vs concentration curves of SDS and CTAB and I_1/I_3 of pyrene fluorescence spectra vs concentration curves of AEO; the recipes and conditions in the preparation of Surfactant@PSNS (PDF)

■ AUTHOR INFORMATION

Corresponding Authors

*Tel.: 86-532-80662750. Fax: 86-532-80662750. E-mail: luosj@qibebt.ac.cn.

*Tel.: 86-532-80662708. Fax: 86-532-80662708. E-mail: guorb@qibebt.ac.cn.

Notes

The authors declare no competing financial interest.

■ ACKNOWLEDGMENTS

This work was supported by the National Natural Science Foundation of China (31101918, 4126143), Key Projects in the National Science and Technology Pillar Program (20140015), Key Research & Development Project of Shandong (No. 2015GSF115037), and Qingdao Science and Technology and People's Livelihood Project (14-2-3-69 nsh).

■ REFERENCES

(1) Sloan, E. D.; Koh, C. A. In *Clathrate Hydrates of Natural Gases*; Heinemann, H., Speight, J. G., Eds.; CRC Press: Boca Raton, 2007; Chapter 2, pp 60−63.

(2) Gudmundsen, J.; Borrehaug, A. Frozen hydrate for transport of natural gas. *Second International Symposium on Gas Hydrates*; Toulouse, 1996; pp 415−422.

(3) Yevi, G. Y.; Rogers, R. E. Storage of fuel in hydrates for natural gas vehicles (NGVs). *J. Energy Resour. Technol.* **1996**, *118*, 209−213.

(4) Mori, Y.; Mochizuki, T. Modeling of mass transport across a hydrate layer intervening between liquid water and guest liquid phases. *Second International Symposium on Gas Hydrates*; Toulouse, 1996; pp 267−274.

(5) Herri, J.; Gruy, F.; Cournil, M. Kinetics of methane hydrate formation. *Second International Symposium on Gas Hydrates*; Toulouse, 1996; pp 243−250.

(6) Zhong, Y.; Rogers, R. E. Surfactant effects on gas hydrate formation. *Chem. Eng. Sci.* **2000**, *55*, 4175−4187.

(7) Zhang, C. S.; Fan, S. S.; Liang, D. Q.; Guo, K. H. Effect of additives on formation of natural gas hydrate. *Fuel* **2004**, *83*, 2115−2121.

(8) Kumar, A.; Bhattacharjee, G.; Kulkarni, B. D.; Kumar, R. Role of Surfactants in Promoting Gas Hydrate Formation. *Ind. Eng. Chem. Res.* **2015**, *54*, 12217−12232.

(9) Watanabe, K.; Imai, S.; Mori, Y. H. Surfactant effects on hydrate formation in an unstirred gas/liquid system: An experimental study using HFC-32 and sodium dodecyl sulfate. *Chem. Eng. Sci.* **2005**, *60*, 4846−4857.

(10) Gayet, P.; Dicharry, C.; Marion, G.; Graciaa, A.; Lachaise, J.; Nesterov, A. Experimental determination of methane hydrate dissociation curve up to 55 MPa by using a small amount of surfactant as hydrate promoter. *Chem. Eng. Sci.* **2005**, *60*, 5751−5758.

(11) Zhang, J. S.; Lee, S.; Lee, J. W. Kinetics of methane hydrate formation from SDS solution. *Ind. Eng. Chem. Res.* **2007**, *46*, 6353−6359.

(12) Ganji, H.; Manteghian, M.; Omidkhah, M. R.; Rahimi Mofrad, H. Effect of different surfactants on methane hydrate formation rate, stability and storage capacity. *Fuel* **2007**, *86*, 434−441.

(13) Okutani, K.; Kuwabara, Y.; Mori, Y. H. Surfactant effects on hydrate formation in an unstirred gas/liquid system: An experimental study using methane and sodium alkyl sulfates. *Chem. Eng. Sci.* **2008**, *63*, 183−194.

(14) Yoslim, J.; Linga, P.; Englezos, P. Enhanced growth of methane−propane clathrate hydrate crystals with sodium dodecyl sulfate, sodium tetradecyl sulfate, and sodium hexadecyl sulfate surfactants. *J. Cryst. Growth* **2010**, *313*, 68−80.

(15) Wang, F.; Jia, Z. Z.; Luo, S. J.; Fu, S. F.; Wang, L.; Shi, X. S.; Wang, C. S.; Guo, R. B. Effects of Different Anionic Surfactants on Methane Hydrate Formation. *Chem. Eng. Sci.* **2015**, *137*, 896−903.

(16) Wang, F.; Guo, G.; Liu, G. Q.; Luo, S. J.; Guo, R. B. Effects of Surfactants Micelles and Surfactant-coated Nanospheres on Methane Hydrate Growth Pattern. *Chem. Eng. Sci.* **2016**, *144*, 108−115.

(17) Zhang, X. X.; Liu, H.; Sun, C. Y.; Xiao, P.; Liu, B.; Yang, L. Y.; Zhan, C. H.; Wang, X. Q.; Li, N.; Chen, G. J. Effect of water content on separation of CO2/CH4 with active carbon by adsorption−hydration hybrid method. *Sep. Purif. Technol.* **2014**, *130*, 132−140.

(18) Linga, P.; Daraboina, N.; Ripmeester, J. A.; Englezos, P. Enhanced rate of gas hydrate formation in a fixed bed column filled with sand compared to a stirred vessel. *Chem. Eng. Sci.* **2012**, *68*, 617−623.

(19) Zhong, D. L.; Daraboina, N.; Englezos, P. Coal Mine Methane Gas Recovery by Hydrate Formation in a Fixed Bed of Silica Sand Particles. *Energy Fuels* **2013**, *27*, 4581−4588.

(20) Wang, W. X.; Bray, C. L.; Adams, D. J.; Cooper, A. I. Methane Storage in Dry Water Gas Hydrates. *J. Am. Chem. Soc.* **2008**, *130*, 11608−11609.

(21) Fan, S. S.; Yang, L.; Wang, Y. H.; Lang, X. M.; Wen, Y. G.; Lou, X. Rapid and high capacity methane storage in clathrate hydrates using surfactant dry solution. *Chem. Eng. Sci.* **2014**, *104*, 53−59.

(22) Wang, F.; Luo, S. J.; Fu, S. F.; Jia, Z. Z.; Dai, M.; Wang, C. S.; Guo, R. B. Methane Hydrate Formation with Surfactants Fixed on the Surface of Polystyrene Nanospheres. *J. Mater. Chem. A* **2015**, *3*, 8316−8323.

(23) Mukerjee, P.; Mysels, K. J. *Critical Micelle Concentration of Aqueous Surfactants Systems*; National Bureau of Standards: Washington, DC: 1971; Vol. *36*.

(24) Desnoyers, J. E.; Perron, G.; Roux, A. H. In *Thermodynamic Methods, Surfactant Solutions, New Methods of Investigation, Surfactant Science Series*; Zana, R., Ed.; Marcel Dekker: New York, 1987; Vol. *22*, pp 2−51.

(25) Pineiro, L.; Novo, M.; Al-Soufi, W. Fluorescence emission of pyrene in surfactant solutions. *Adv. Colloid Interface Sci.* **2015**, *215*, 1−12.

(26) Wang, F.; Fang, K. Effect of molecular structures of Gemini and polymerizable emulsifiers on cationic emulsion copolymerization of styrene and butyl acrylate. *Colloid Polym. Sci.* **2014**, *292*, 1449−1455.

(27) Gutt, C.; Asmussen, B.; Press, W.; Johnson, M. R.; Handa, Y. P.; Tse, J. S. The structure of deuterated methane−hydrate. *J. Chem. Phys.* **2000**, *113*, 4713.
(28) Makogon, Y. F. *Hydrates of Hydrocarbons*; Pennwell Books: OK, 1997; p 36.
(29) Smith, J. M.; Van, N. H. C.; Abbott, M. M. In *Introduction to Chemical Engineering Thermodynamics*; McGraw-Hill Education: Singapore, 2001; pp 96−98.
(30) Wang, F.; Wang, L.; Wang, C. S.; Guo, G.; Liu, G. Q.; Luo, S. J.; Guo, R. B. Direction controlled methane hydrate growth. *Cryst. Growth Des.* **2015**, *15*, 5112−5117.
(31) Aguiar, J.; Carpena, P.; Molina-Bolıvar, J. A.; Carnero Ruiz, C. On the determination of the critical micelle concentration by the pyrene 1 3 ratio method. *J. Colloid Interface Sci.* **2003**, *258*, 116−122.
(32) Sloan, E. D.; Koh, C. A. In *Clathrate Hydrates of Natural Gases*; Heinemann, H., Speight, J. G., Eds.; CRC Press: Boca Raton, 2007; Chapter 2, pp 113−114.

DOI: 10.1021/acssuschemeng.5b01557
ACS Sustainable Chem. Eng. 2016, 4, 2107−2113